SEMARAK ILMU PUBLISHING

Journal of Advanced Research in Applied Mechanics

Journal homepage:
https://semarakilmu.com.my/journals/index.php/appl_mech/index
ISSN: 2289-7895

Hot Embossing of Micro Grating and Its Replication Accuracy

Muhammad Syahrir bin Ahmad[1,2], Ahmad Rosli bin Abdul Manaf[1,*]

[1] Faculty of Manufacturing & Mechatronic Engineering Technology, Universiti Malaysia Pahang Al-Sultan Abdullah, 26600, Pekan, Pahang, Malaysia
[2] Faculty of Manufacturing Engineering Technology, University College TATI, Teluk Kalong, 24000 Kemaman, Terengganu, Malaysia

ARTICLE INFO

Article history:
Received 21 September 2023
Received in revised form 23 November 2023
Accepted 11 December 2023
Available online 13 January 2024

Keywords:
Hot embossing; micro grating; response surface method

ABSTRACT

The Hot Embossing (HE) process was applied in the fabrication of micro grating. High-density polyethene (HDPE) was used as a specimen material for producing microstructure components and parts. In this research, a series of experiments were conducted using an HDPE specimen and embossed the polymer under different parameters such as temperature, embossing time, and embossing force as factors. The experimental setup was based on a response surface method (RSM) that employed a face composite design. The constructed RSM quadratic models assisted in analysing the response parameters, namely accuracy and surface roughness, to determine the relevant linkages between the input variables and the replies. The results defined that hot embossing temperature and hot embossing force will enhance the accuracy and surface quality of the micro grating. Based on RSM, the results revealed that the optimal parameters were as follows: hot embossing temperature is 1650c, embossing force is 10kN/s, and embossing holding time is 150 seconds. Under this condition, the actual deviation of accuracy and surface roughness is 5,75% and -1.32% respectively compared to the actual size of the micro grating mould. Hence, it is highly agreed with the model prediction value. In conclusion, optimization of process parameters on the hot embossing system that was developed is promising to fabricate the HDPE micro grating substrate with optimum dimensional accuracy and surface quality.

1. Introduction

The application of polymer microfabrication techniques nowadays is essential, as an alternative method and cost-effective material instead of traditional materials like silicon or glass. Microfabrication of polymer microstructures using hot embossing (HE) is a flexible and inexpensive technique that involves replicating an embossing master to generate a polymer substrate via micromachining [1,2].

Hot embossing is a method that transfers micro-patterns from a mould to a polymer substrate by heating the polymer workpiece over the glass transition temperature (Tg) and applying optimal

* *Corresponding author.*
E-mail address: arosli@umpsa.edu.my

https://doi.org/10.37934/aram.113.1.118137

pressure to the mould. Figure 1(a) and 1(b) depicted the hot embossing setup and the fluctuation of temperature and pressure during the process.

The advancement of embossing technology as a replication process is then enhanced by numerous researchers and innovations. One of the recent polymer materials recently explored by several researchers is high-density polyethylene (HDPE) to produce optical microlenses HDPE is a cost-effective polymer that substitutes expensive materials like germanium (Ge) and silicon (Si) and is recognized as one of the polymer materials used to produce high-precision and high-quality features on the micro/nanoscale product [3-9].

The most significant way to improve replication accuracy in hot embossing is to identify its optimal parameters. The embossing temperature, demolding temperature, embossing force, holding time, embossing velocity, and demolding velocity are reported as the major HE variable parameters that can be altered by the user due to material and manufacturing behaviour [10,11]. C.Y Chang *et al*., [13] and Deshmukh *et al*., [14] concluded that the impacts of these variable parameters lead to process performance improvements in HE temperature and forces. However, compared to an individual approach, a well-structured multifactor analysis may provide a clearer and more in-depth comprehension of finding the experiment variables and optimal parameters of HE [14-16]. According to Deshmukh *et al*., [14] and Kuo *et al.,* [17] the use of a nonlinear method such as the Design of Experiments (DoE) is useful for investigating the interaction effects of HE factors. Lan *et al*., [15] used the L9 Taguchi technique to determine the most influential HE factors, which are then examined using ANOM and ANOVA. They found that the temperature is the most significant factor that affects the form accuracy, this finding is similar to the investigation done by Kuo *et al*., [17]. Meanwhile, a conventional experiment method was used by He *et al*., [18], Wu *et al*., [19], and Moore *et al*., [16] in which these researchers conducted a series of experiments and discovered that the significance of temperature level contributes to an increasing percentage of shrinkage on the specimen geometry. Based on the previous literature, HE temperature, HE forces and holding time are the essential process parameters for hot embossing. However, the result of their experiments has not thoroughly and systematically investigated the relationship between process parameters and the final quality of HDPE substrate using DOE.

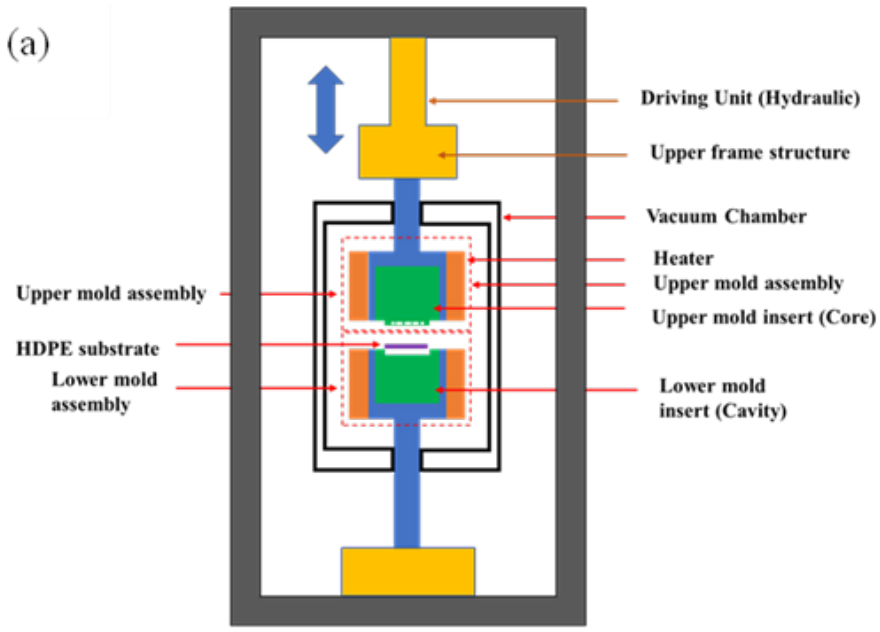

(a)

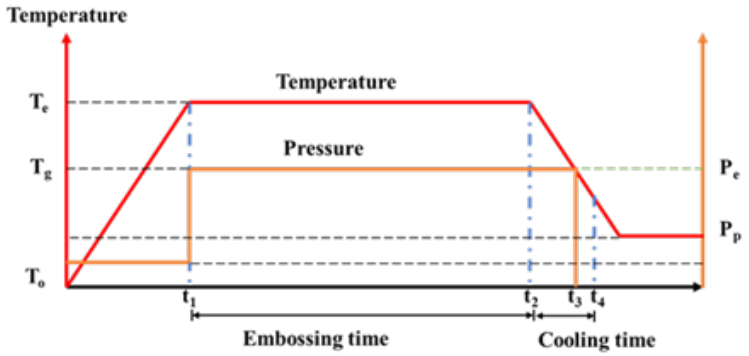

(b)

Fig. 1. Schematic representation of the (a) hot embossing process setup and (b) variation of hot embossing parameters

This paper's present study utilised RSM approaches to investigate the influence parameters on the HDPE micro grating substrate accuracy and surface quality using non-vacuum conditions with different process parameters and approaches. The current investigation makes use of Design Expert software, and the tests are mapped out with the use of a face-centered design (FCD) method. Twenty experiments were performed using the FCD as a procedure. The HE temperature, HE forces and HE holding time are chosen as the response factors while in RSM evaluation. The influence of the variable parameters on the HDPE micro grating substrate will be analysed and validated through RSM and the optimal parameters for fabricating the substrate will be identified.

2. Experiment Procedure

2.1 Mould Design

A concept of mould design follows the basic concept of the hot embossing process. The upper and lower mould has been designed by using CAD software as shown in Figure 2(b). It was designed specifically to achieve this research outcome. The mould material used is aluminium alloy 6061 which had advantages in strength-to-weight ratio, malleability, and machineability [4,6,7,20]. This material had adequate strength to avoid mould deflection throughout the embossing process on the HDPE sheet.

The upper and lower mould was set to 50 mm diameter, the upper mould is designed with a 25mm diameter circular pocket for attaching the micro grating insert. The lower mould pocket is 30 mm, space to assemble the lower mould insert. Meanwhile, the height of both moulds is 70 mm to ensure that it can be attached to the upper plate of the universal testing machine (UTM). The upper mould was built with a circular shape holder to secure the mould to the UTM machine. To ensure the mould can be heated to the required temperature, a circular ring heater was attached. The size of the heater dictates that the diameter of the mould is 50 mm. The drawing of the mould is depicted in Figure 2. The heater was attached to the upper and lower mould in which the temperature is controlled by the PID controller. The minimum temperature is 10^{o}C while the maximum temperature is 500^{o}C.

2.2 Insert Design and Fabrication

The mould inserts with micro grating features were designed and fabricated using aluminium 6061-T6. The 6061-T6 designation denotes the temper or level of hardness, which is attained by the process of precipitation hardening. This grade exhibits a favourable strength-to-weight ratio and can

be subjected to heat treatment. The size of the lower insert is diameter 30 mm x 30 mm thickness and the upper insert size is diameter 30 mm x 25 mm thickness. The insert is fabricated using the turning machine for cylinder shape and the CNC milling machine to fabricate micro grating features. The upper insert consists of protrusion with a diameter of 15 mm and 2 mm in height, while the lower insert has a pocket with a diameter of 15.5 mm and 1 mm in height.

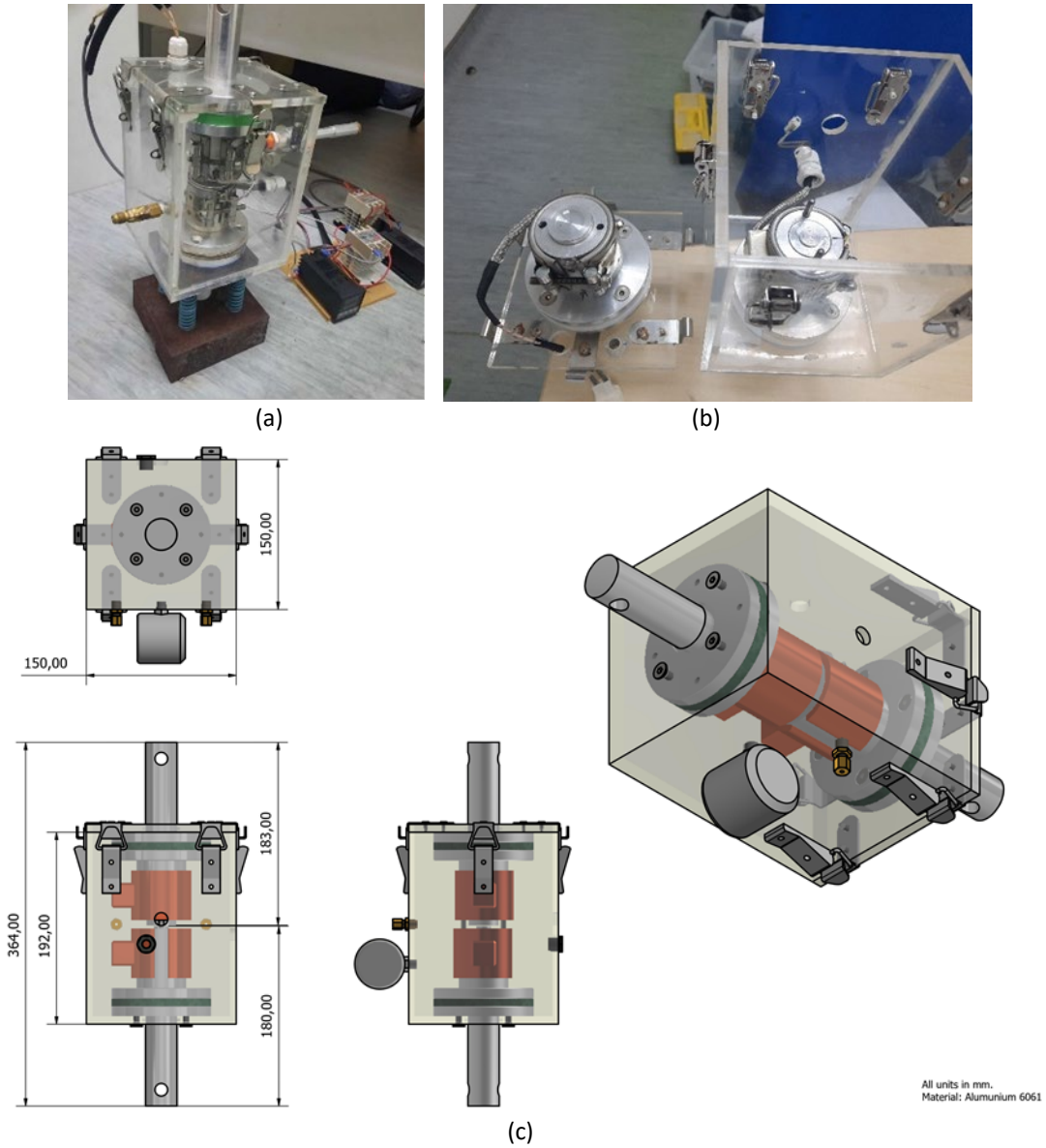

Fig. 2. Photograph of HE moulds (a) Mould assembly (b) Mould Insert and (c) Mould assembly drawing

As shown in Figure 3 the schematic view of the upper and lower insert. Meanwhile, Figure 4(a) shows the fabricated lower mould and Figure 4(b) shows the upper mould insert with the micro grating structure on top of the insert. The grating insert is machined using an endmill cutter diameter of 0.50 mm with the cutting speed set to 3000 rpm while the feed rate is at 0.5 mm/min.

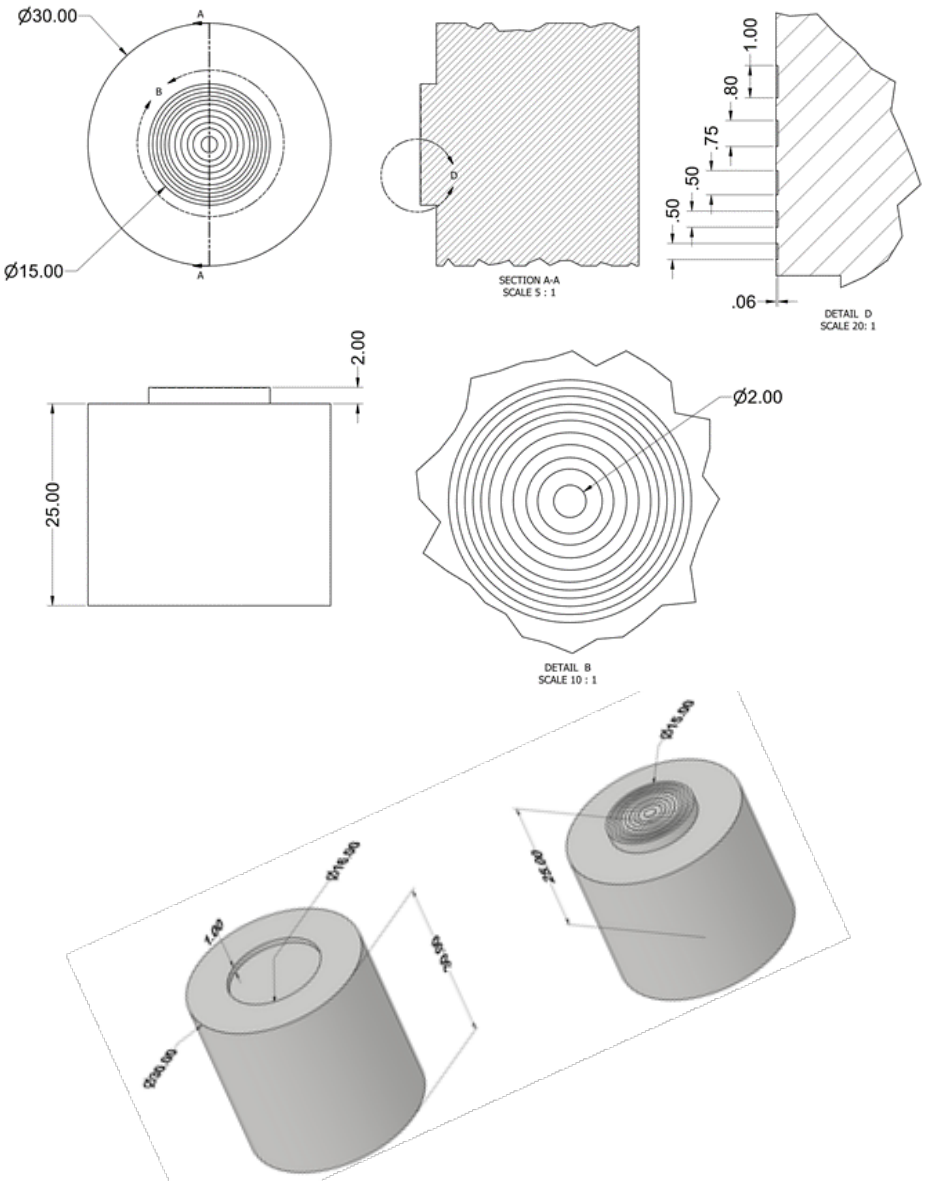

Fig. 3. Schematic diagram of mould insert

(a) (b)

Fig. 4. Fabricated moulds insert (a) Lower mould and (b) Upper mould

The selected test specimen material is high-density polyethene (HDPE). It is opaque and solid to withstand higher temperatures around 120 Celsius. It comes in a substantial size, hard to comprehend but it is a very well-known material with other magnificent advantages. During embossing, HDPE polymer was placed on top of the lower mould and under the upper mould as a test specimen as shown in Figure 5(b). This specimen functioned as a patterned material in which micro grating structures are formed. Figure 5(a) shows the detailed dimensions of the actual HDPE specimen [6,21]. The details properties of HDPE are in Table 1.

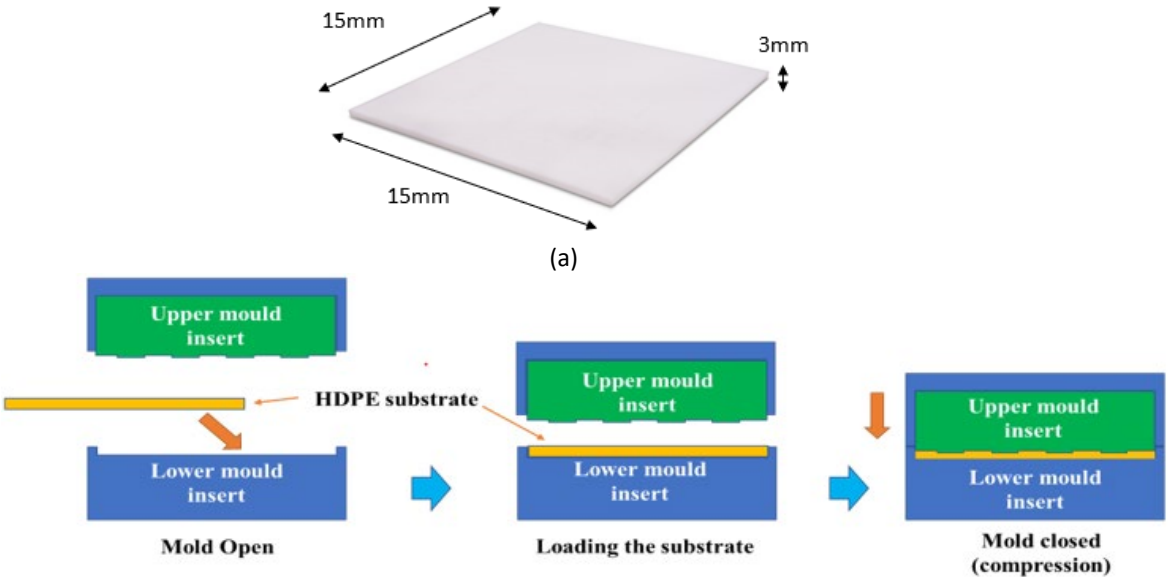

Fig. 5. Detail of the HDPE specimen (a) substrate dimension and (b) schematic diagram of substrate load into a mould

Table 1
Properties of HDPE

Material Properties	Value
Density, g/cm3	0.930 – 0,955
Melting point, (^{o}C)	210 – 270 ^{o}C
Softening point, (^{o}C)	0.1 to 100
Material shape	Sheet
Material thickness, (mm)	3
Refractive index	-

2.3 Embossing Process

In this study, the micro grating replication process is carried out utilising a customized Universal Testing Machine (UTM) INSTRON 3369, with the mould assembly mounted to the machine's load frame (see Figure 6 (a)-(b)). In both embossing and compression, the substrate is pressed down using an upper mould that is fastened to a load frame. In addition, the machine's feed and depth of substrate may be controlled in real-time throughout an experiment. The mould assembly was fastened in place on top of the Instron load frame. At the same time, the bottom mould will be fastened to the foundational structure. The machine's location, embossing process monitoring, data collecting, and report generation were all managed by a program called Bluehill 2.

As shown in Figure 6 (b) below, the mould had been attached with thermocouples, heaters, a locking system, and a temperature control system. The mould assembly is covered by an acrylic box to avoid ambient air and dust entering the mould space. The air-cooling gun is used to blow fresh air after the embossing process. Each substrate will be cooled from 100 to 200 seconds before the demoulding process.

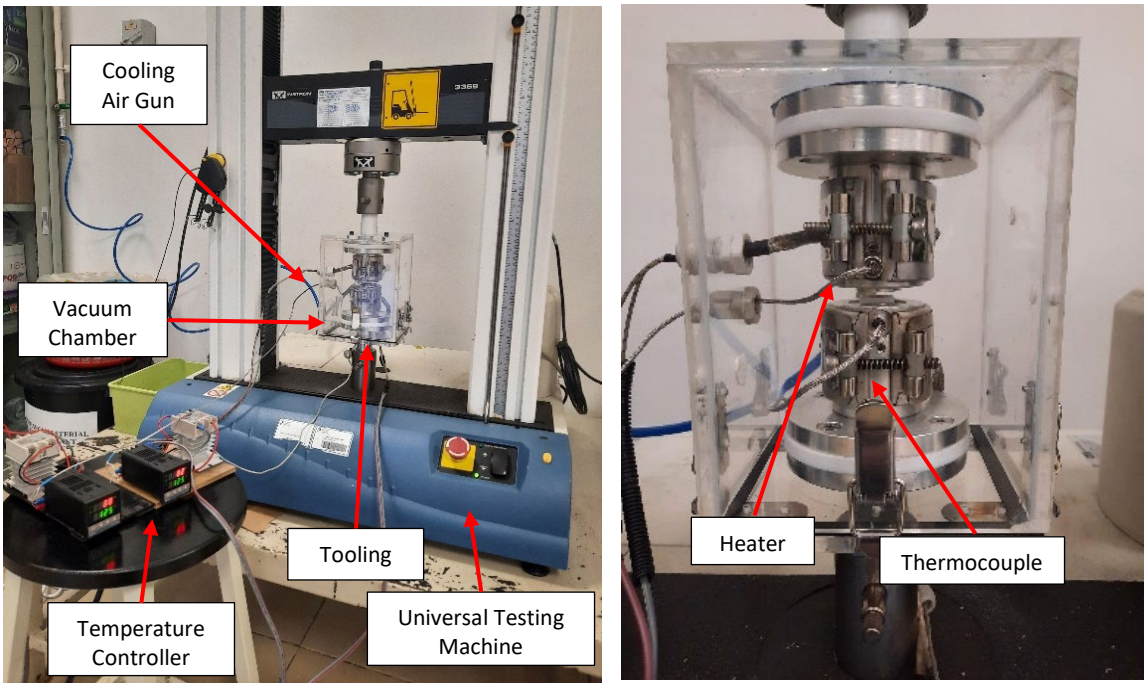

(a) (b)

Fig. 6. (a) Hot embossing process setup (b) Heating system

The movement and pressure of the mould were controlled and monitored by the UTM machine. To avoid heat from heaters being transferred to the UTM, 2 pieces of Teflon plates were used and attached to a mould as a thermal resistance material. The input of the experiment parameters is embossing temperature, force, and embossing time were selected and the experiment steps were designed using RSM as depicted in Table 3.

2.4 Replication Accuracy and Surface Evaluation

The micro grating substrate specimens were examined by using a three-dimensional (3D) laser microscope named LEXT OLS5000 Olympus for the replication accuracy and surface roughness evaluation as shown in Figure 7. Figure 7(a) shows the non-contact measurement technique is chosen to avoid damage to the specimen. The data of micro grating dimensional size and surface roughness is (Figure 7(a)-(b)) recorded to gain the data of each specimen. Furthermore, the specimen data is calculated and compared with the measurement data of the mould insert that was measured earlier. Figure 8 shows the image captured from the 3D microscope for dimensional and surface roughness measurement.

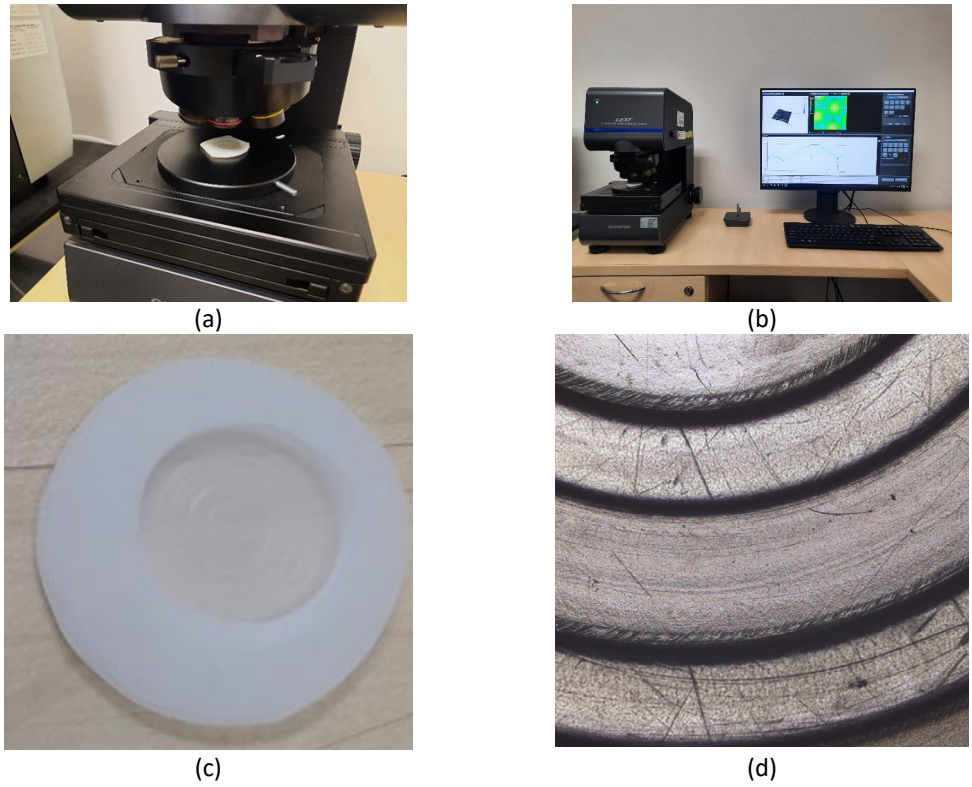

(a) (b)

(c) (d)

Fig. 7. Replication accuracy and surface roughness evaluation of the micro grating substrate. (a) Sample measurement (b) analysis process (c) HDPE micro grating specimen and (d) Image of a specimen from Lext OLS5000

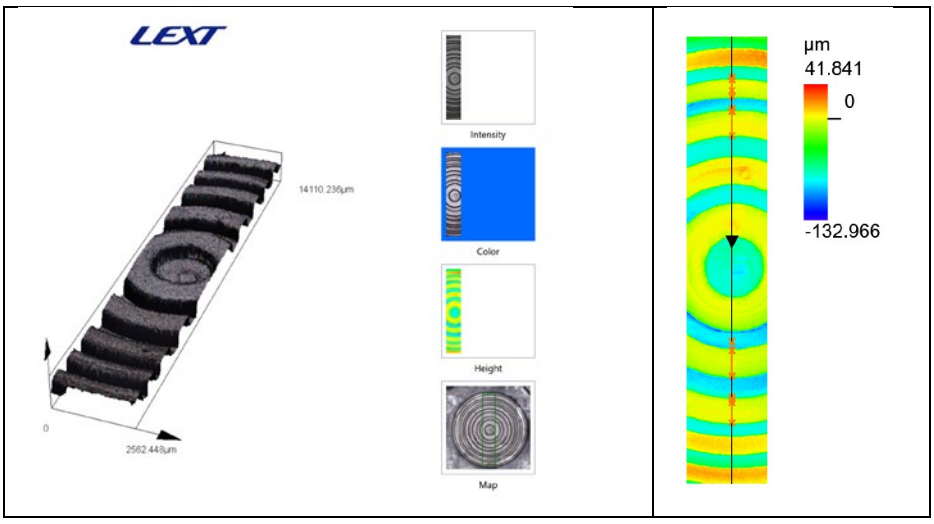

Fig. 8. An image captured by the 3D laser microscope

3. Experimental Design using RSM

In the current study, three separate experimental variables were important determinants in the accuracy and surface roughness as responses. These factors were the temperature, the force, and the holding duration. Each component in a model-fitting design must have at least three distinctive levels. The requirement is met by central composite designs (CCDs) with three levels per variable. The face-centered design (FCD) is centered and scaled to (+1, +1, +1) with = 1 since the area of operability and region of concern are almost identical. For this investigation, FCD was used to acquire

experimental data that would be consistent with complete second-order polynomial models defining response surfaces across a wide range of parameters. Eq. (1) is used in CCD to calculate the number of experiment points.

$$N = 2^n + 2_n + n_0 \tag{1}$$

where *N* is the number of the running test of the experiment, *n* is the number of factors and n_0 is the number of central points. As Eq. (1) shows, the ''2^n'' term is known as factorial experiment points. These points permit approximations of all important causes and 2-factors interrelations between two components. Meanwhile, the axial point term is known as ''2_n'' which permits the estimation of pure quadratic effects. Lastly, ''n_0'' represents the center point and can be designed to be run simultaneously both as factorial points and axial.

Each variable was separated into three categories: high (+1), low (-1) and centre points (coded level as 0). FCD with three factors had a total of 20 runs of trials in this investigation, with eight factorial points, six axial points, and six central points. It was utilised to analyse the experimental work's outcomes. Table 2 shows the whole experimental design, including coded and actual numbers, as well as the maximum and minimum temperatures, forces, and holding periods. Multiple regression analysis was used to calculate the coefficients. The RSM method creates a model for each dependent variable, with the main and interaction effects of each variable represented individually [22]. The multivariate model is denoted by Ferreira *et al.*, [23]

$$Z = \beta_0 + \sum_{i=1}^{3} \beta_i x_i + \sum_{i=1}^{3} \beta_{ii}\, x_i x_i + \sum_{i=1}^{3} \beta_{ij} x_i x_j \tag{2}$$

Table 2
Denote a list of hot embossing input variables and levels

Embossing parameters	Level 1	Level 2	Level 3
Embossing Temperature (°c)	155	160	165
Embossing Pressure (kN/s)	5	10	15
Embossing Time (Seconds)	100	150	200

3.1 Optimization via Desirability Approach

Response surface methodology (RSM) uses the desirability approach to optimise more than one response variable at the same time. It means giving each response variable a desirability value based on its target value and acceptable range. The desirability function then adds these values together to make an overall measure of desirability that can be used to find the best settings for the variables that were given as input. The optimisation approach required transforming each response to a dimensionless desire value between 0 and 1 using the Design Expert software. The response is extremely unsatisfactory since the dimensionless value of *d* = 0, but the response is extremely desired since *d* = 1. In the current study, each reaction has a distinct goal, either to maximise or minimise. Using a geometric approach, the response desirability is then integrated to produce the final total general desirability, *D*. The mathematical model derived by Derringer and Suich's *et al.*, [23] for the Desirability Approach is provided in Eq. (3).

$$D = (d_1 \times d_2 \times \ldots \times D_n)^{1/n} = (\prod_{i=1}^{n} d_i)^{1/n} \tag{3}$$

The single value of *D* gives the overall value of desirability. The d_i ranges from $0 \leq d_i \leq 1$ (least to most desirable, respectively), represents the desirability of each (*i*) response and *n* is the number of responses being optimized.

Table 3
The experimental design, result, and prediction based on RSM

Run	Process parameters setting			Response				Deviation	
	Embossing Temperature (°C)	Embossing Force (kN/s)	Embossing Holding Time (s)	Depth accuracy (μm) (Average)	Surface Roughness (Ra) (Average)	Depth accuracy (%)	Surface Roughness (%)	Depth accuracy (%)	Surface Roughness (%)
1	160	10	150	59.531	35.060	91.14%	107.34%	8.86%	-7.34%
2	165	5	200	59.795	30.748	91.55%	94.14%	8.45%	5.86%
3	160	10	150	59.707	35.488	91.41%	108.65%	8.59%	-8.65%
4	160	5	150	58.163	37.069	89.05%	113.49%	10.95%	-13.49%
5	155	15	200	55.809	36.867	87.42%	112.87%	12.58%	-12.87%
6	160	10	100	57.626	36.756	88.23%	112.53%	11.77%	-12.53%
7	165	10	150	61.561	33.093	94.25%	101.32%	5.75%	-1.32%
8	165	15	100	60.022	34.155	91.89%	104.57%	8.11%	-4.57%
9	160	10	150	58.775	34.371	89.99%	105.23%	10.1%	-5.23%
10	160	15	150	59.340	33.324	90.85%	102.02%	9.15%	-2.02%
11	160	10	150	59.919	35.581	91.74%	108.93%	8.26%	-8.93%
12	155	5	100	52.746	41.926	80.76%	128.36%	19.24%	-28.36%
13	165	15	200	60.115	30.884	92.04%	94.55%	7.96%	5.45%
14	160	10	200	61.386	32.068	93.98%	98.18%	6.02%	1.82%
15	160	10	150	60.279	36.015	92.29%	110.26%	7.71%	-10.26%
16	155	10	150	53.661	37.601	82.16%	115.12%	17.84%	-15.12%
17	165	5	100	59.453	33.905	91.02%	103.80%	8.98%	-3.80%
18	155	15	100	54.873	41.145	84.01%	125.97%	15.99%	-25.97%
19	160	10	150	60.298	35.273	92.32%	107.99%	7.68%	-7.99%
20	155	5	200	55.244	37.300	84.58%	114.20%	15.42%	-14.20%

Deviation in-depth = (Depth of positive micro-channel – Channel of aluminium mould) - (depth of embossed microchannel); Depth of positive feature micro-channel over aluminium mould= 65.316μm
Deviation in surface roughness = (Surface roughness of positive micro-channel – Channel of aluminium mould) - (Surface roughness of embossed microchannel); Depth of positive feature micro-channel over aluminium mould= 32.663μm (Ra)

4. Result, Analysis and Discussion

4.1 Experimental Result

The present study focuses on investigating the factors that influenced the quality of the replication accuracy and surface roughness of embossed microchannels by adjusting the parameters of the hot embossing process. This experiment was carried out utilizing a face-centered design (FCD) with experimental factors namely temperature, force, and holding time. With three factors ($n = 3$) and six central points ($n_0 = 6$), The experiment requires twenty repetitions. These parameters have been designated at three levels and the statistical model table (with 20 runs) is defined by the number of parameters and their levels as discussed by Chen *et al.*, [1]. Table 3 summarizes the design matrix and their related points on fitted models based on RSM.

Hence, all successful experiments related to the hot embossing process were defined. It mainly examines all the results and discussion of the conducted experiment through surface integrity evaluation. The results obtained will be used to evaluate the replication accuracy of micro grating due to different parameters such as temperature, embossing force, and embossing time. The replication accuracy of an embossed micro-channel is calculated using Eq. (4).

$$Replication\ Accuracy = \frac{Size\ of\ micro\ grating\ features\ on\ substrate}{Size\ of\ positive\ feature\ of\ grating\ mould} \quad (4)$$

4.2 Analysis of Data

The following subsections describe the analysis of response data (force, temperature, and holding time) employing analysis of variance (ANOVA) and the response surface method. ANOVA is performed using the Design Expert software. Utilising the collected data, the software ensures statistical accuracy and generates a response model equation. For any ANOVA, the normal probability plot must be evaluated for the range of residuals, which should be near the mean line [24,25]. As normal probability diagrams, Figure 9(a)-(b) depicts the results of the normality test for the experimental findings. This test was performed on the results of the experiment. The figures compare the numbers that were predicted to those that were achieved for the design matrix. Consequently, as the mean line is frequently fitted for all responses, Figure 9(a)-(b) demonstrates that the residual values are modest and closely aligned with the mean line.

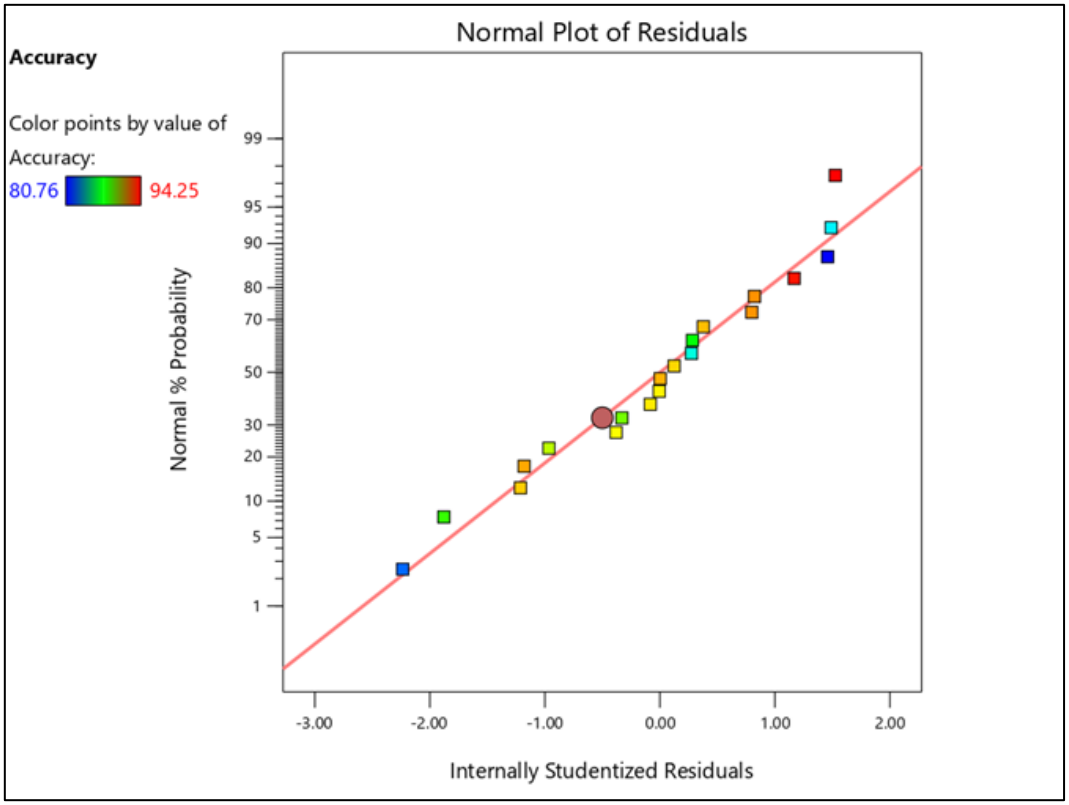

(a)

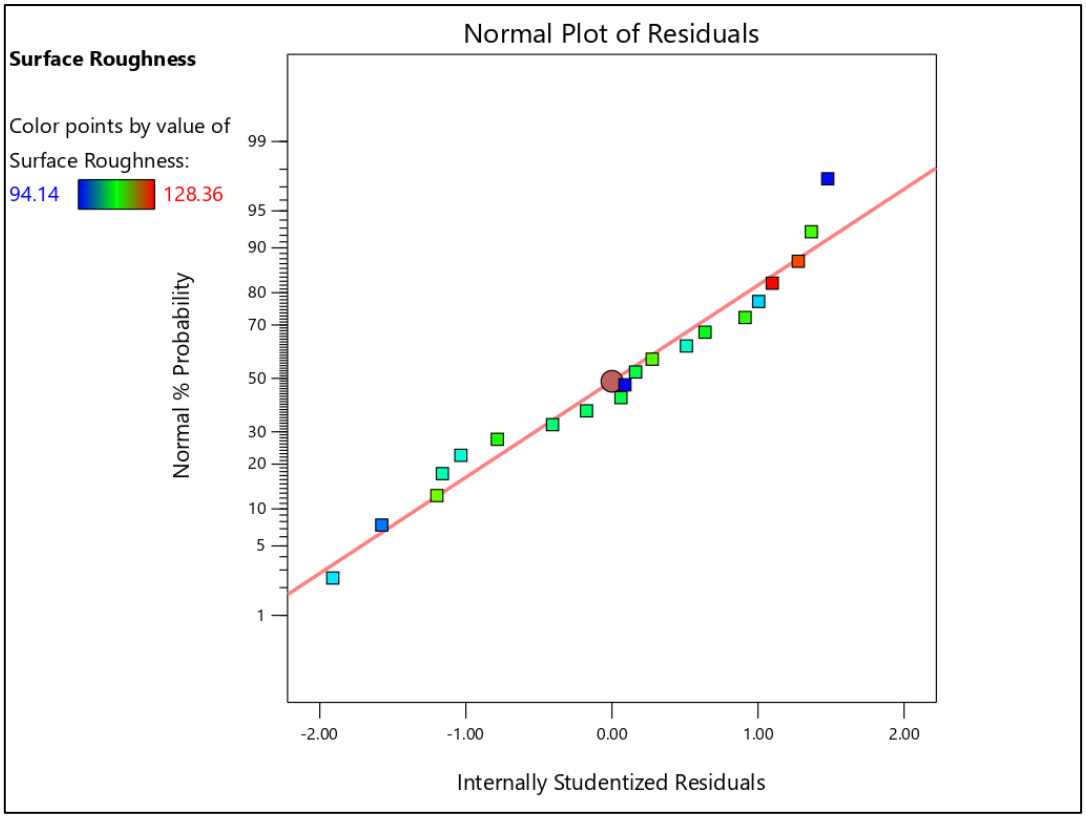

(b)

Fig. 9. Normal probability plot of (a) accuracy and (b) surface roughness

4.3 Impact of Embossing Parameters on Replication Accuracy

As shown in Figure 9, a 3D response surface and 2D contour plots were used to analyze the interaction effects of two variables on the accuracy of the micro grating substrate' geometries based on the regression equation. When the shape of the contour plot is elliptic instead of round, the interaction between variables is significant. Otherwise, the interaction is insignificant. Besides, when the shape of the response surface is convex, the range of variables was set reasonably as per set up by Chen *et al.*, [22]. The results of the analysis of variance (ANOVA) for accuracy response and the summary of a quadratic model are shown in Table 4. The coefficient of determination R^2 for accuracy is 0.9315. The model described 93.15 per cent of the response variability. In addition, Table 4 demonstrates that the projected *R*-squared value is 0.5692, which is consistent with the predicted R-squared value of 0.8698. The adequate precision value is 13.2255 which is signal to noise ratio greater than 4 is desirable. Furthermore, the *f* value is 15.10 which shows that the model is significant. In terms of factors, temperature (*A*), holding time (*C*) and *A2* show significance with *P*-values of less than 0.05. Other models are not significant with *P*-values, which its value is more than 0.100. Nevertheless, the "Lack of Fit" for the *f* value is 4.11 means it is not as significant as required due to the value being larger than 0.1000. The developed quadratic model for accuracy as fitted based on RSM in terms of the experimental factors determined by Eq. (5) and was a closed margin to the experimental values.

$$accuracy = -2922.47868 + 36.00197A + 4.78461B + 0.530125C - 0.023650AB - 0.003275AC - 0.000395BC - 0.107618(A^2) - 0.037818(B^2) + 0.000084(c^2) \quad (5)$$

where *A* is the temperature in (^{0}C), *B* is the force (kN/s) and *C* is holding time. In the equation, a positive sign for the coefficient suggests a synergistic outcome, whereas a negative sign implies an antagonistic influence on the measured response [18].

Table 4
Model summary and ANOVA for the accuracy response in the quadratic model

Source	Model Summary	Sum of squares	*df*	Mean squares	*f* value	*p*-value prop > *f*	Remarks
R^2	0.9315	-	-	-	-	-	-
Adjusted R^2	0.8698	-	-	-	-	-	-
Adequate precision	13.2255	-	-	-	-	-	> 4
Predicted R^2	0.5692	-	-	-	-	-	Closed to adj R^2
Model	-	261.92	9	29.10	15.10	0.0001	Significant
A-Temperature	-	174.89	1	174.89	90.73	< 0.0001	
B- Force	-	8.56	1	8.56	4.44	0.061	
C- Holding time	-	18.66	1	18.66	9.68	0.011	
AB	-	2.80	1	2.80	1.45	0.256	
AC	-	5.36	1	5.36	2.78	0.126	
BC	-	0.0780	1	0.09	0.04	0.844	
A^2	-	19.91	1	19.91	10.33	0.009	
B^2	-	2.46	1	2.46	1.28	0.285	
C^2	-	0.1208	1	0.12	0.06	0.807	
Residual	-	19.28	10	1.93			
Lack of fit		15.51	5	3.10	4.11		Not Significant
Pure error		3.77	5	0.7540			

Based on ANOVA, the temperature of hot embossing reflects a significant interaction with some of the factors. The effects of Hot embossing temperature, hot embossing force, and their influence on the accuracy value of micro grating substrate are revealed in Figure 10. The accuracy of the micro grating profile increased gradually when the HE temperature increased in the range of 155-165^{o}c, and the force increased in the range of 5 to 15 kN and then the accuracy value increased from 80.76 to 94.25%. The viscosity of the polymer is reduced as the temperature rises, enhancing the filling of HDPE into the cavities, as per discussed by Li *et al.*, [12] and Deshmukh *et al.,* [26].

According to the results in Table 3, the circular contour patterns in Figure 10 (b) demonstrated that there was no significant relationship between the interaction of the embossing force and temperature. This is also supported by Eq. (5). A maximum accuracy value (94.25%) of the micro grating was obtained when the HE temperature was approximately 165^{0}c and the HE forces value at 10kN.

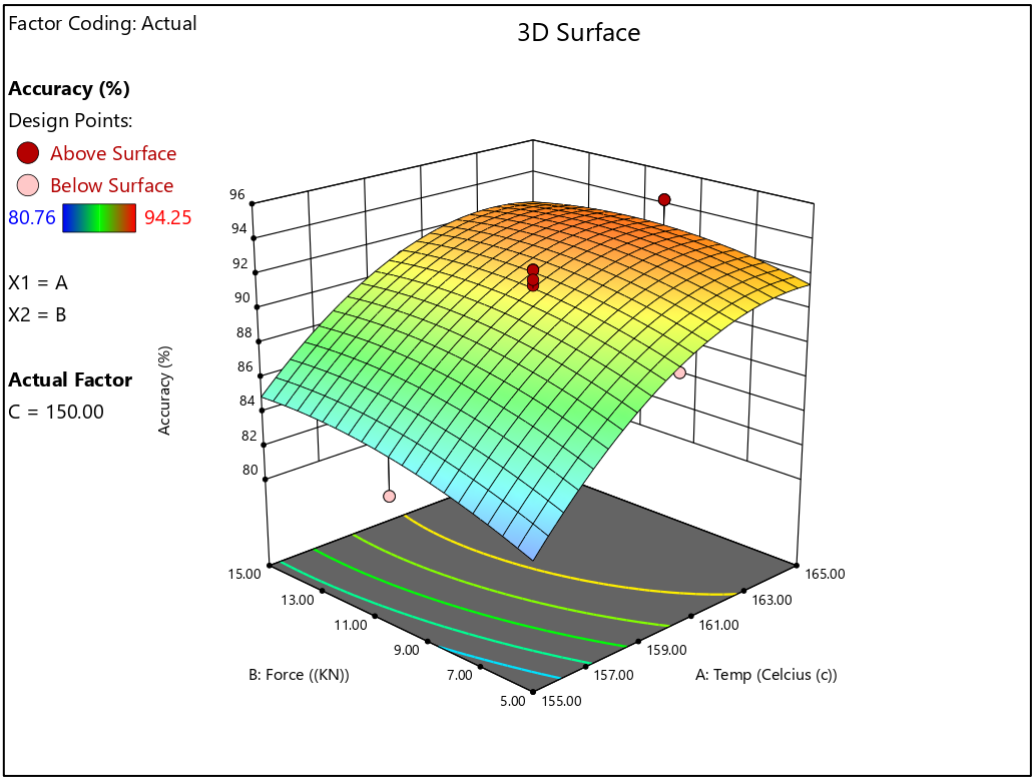

(a)

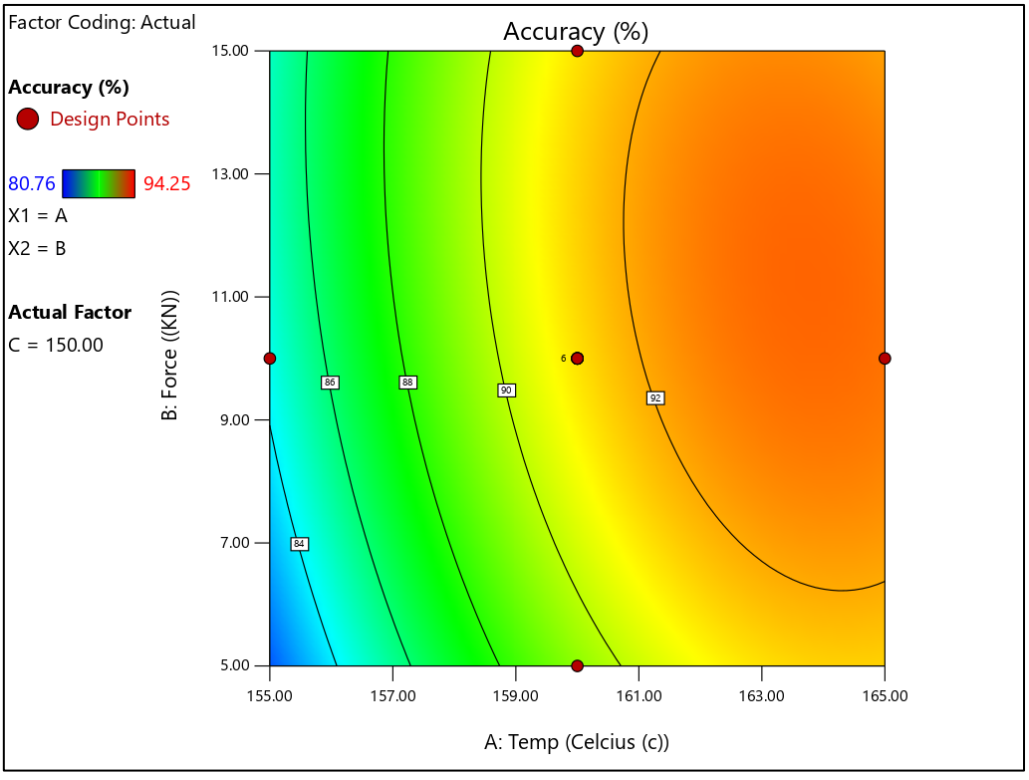

(b)

Fig. 10. Influence of temperature and force on the accuracy of HDPE substrate (a) 3D surface plot (b) contour plot

4.4 Impact of Embossing Parameters on Replication Surface Roughness

Table 5 illustrates the model summary of the quadratic model and the analysis of variance (ANOVA) for surface roughness. The regression models had a high *F*-value (19.56) and a low p-value (0.0001), both of which indicated the model is significant. The model could be used to estimate the surface roughness percentage of the micro grating substrate because the lack of fit (*F*-value = 4.80, *p*-value = 0.0531 > 0.05) was statistically it is not significant. According to Table 5, the fit of the model was also expressed in the coefficient of determination as R^2. The value point indicates that the surface roughness model can explain 0.9343 (93.43%) of the response variability. Askins *et al*., [27] summarized that the better the models fit the experimental data, the closer the R^2 value is to 1. Both the determination coefficient (R^2 = 0.9343) and the adjusted determination coefficient (*Adj* R^2 = 0.8866) were significant and the difference between these values is less than 0.2 as desired, indicating that the anticipated and experimental values were correlated. The reliability and precision of the experimental data were shown by the low percentage coefficient of variation (C.V.) (2.75%) and high Adeq. precision (17.335). Moreover, the significance of each coefficient can be determined using the *F*-value (which is positively correlated with significance) and *p*-values (negatively correlated with significance). When the model's *p*-value was less than 0.05, it was statistically significant and suitable for optimizing the extraction parameters. Significant were the independent variables (A-Temp and B-Holding time), however, the remaining coefficients (AB, AC, and BC) were not statistically significant. As fitted using RSM and the experimental factors, the derived actual quadratic models of surface roughness are displayed in Eq. (6).

$$Surface\ roughness = 0253.57612 - 21.23230A - 5.03421B - 0.732480C + 0.024500(AB) + 0.003790(BC) + 0.000350(BC) + 0.057675(A^{2)} + 0.039075(B^2) \quad (6)$$

where *A* is the hot embossing temperature (°C), *B* is the hot embossing force (kN/s), and *C* is the hot embossing holding time(s). If the coefficient in the equation has a positive sign, it will produce a synergistic result; if it has a negative sign, it will have an antagonistic influence on the response being studied. Eq. (6)'s predicted value for surface roughness (%) was sufficiently close to the experimental values.

Based on ANOVA, hot embossing temperature shows a significant interaction effect with the rest of the variables. The surface roughness percentage gradually decreased or closed to the mould surface roughness with the increment of HE temperature. This is mainly due to the temperature plays a significant role in determining the surface roughness in hot embossing. Increasing the temperature during embossing leads to a decrease in surface roughness (*Ra*). The elevated temperatures increased the viscosity of polymer, thermal expansion of the polymer allowing it to flow and conform to the shape of the mould. Appropriate temperatures lead to increased polymer flow, fill in gaps or defects in the mould and result in a smoother surface [6,18,27,28]. The influence of temperature and force on surface roughness is shown in Figure 11. The curvatures of plots indicate the interaction between the variables as shown in Figure 11 (b). Increasing temperature and force have caused a significant decrease in surface roughness. The optimum parameters that contributed to optimum surface roughness quality that was close to the mould roughness were gained from run number 7.

Table 5
Model summary and ANOVA for surface response surface quadratic model

Source	Model summary	Sum of squares	*df*	Mean squares	*f* value	*p* value prop > *f*	Remarks
R^2	0.9116	-	-	-	-	-	-
Adjusted R^2	0.8950	-	-	-	-	-	-
Predicted *R2*	0.6543	-	-	-	-	-	Clo. to adj *R2*
Adequate precision	27.0315	-	-	-	-	-	-
Model	-	1392.28	8	174.04	19.56	< 0.0001	Significant
A-Temperature	-	963.15	1	963.15	108.25	< 0.0001	Significant
B- Force	-	19.63	1	19.63	2.21	0.1656	
C- Holding time	-	375.65	1	375.65	42.211	< 0.0001	Significant
AB	-	3.00	1	3.00	0.3373	0.5731	
AC	-	7.18	1	7.18	0.8072	0.3882	
BC	-	0.06	1	0.06	0.0069	0.9354	
A^2	-	6.65	1	6.65	0.7477	0.4057	
B^2	-	3.05	1	3.05	0.3432	0.5698	
Residual	-	97.87	11	8.90			X Significant
Lack of fit	-	83.40	6	13.90	4.80	0.0531	
Pure error	-	14.40	5	2.90			

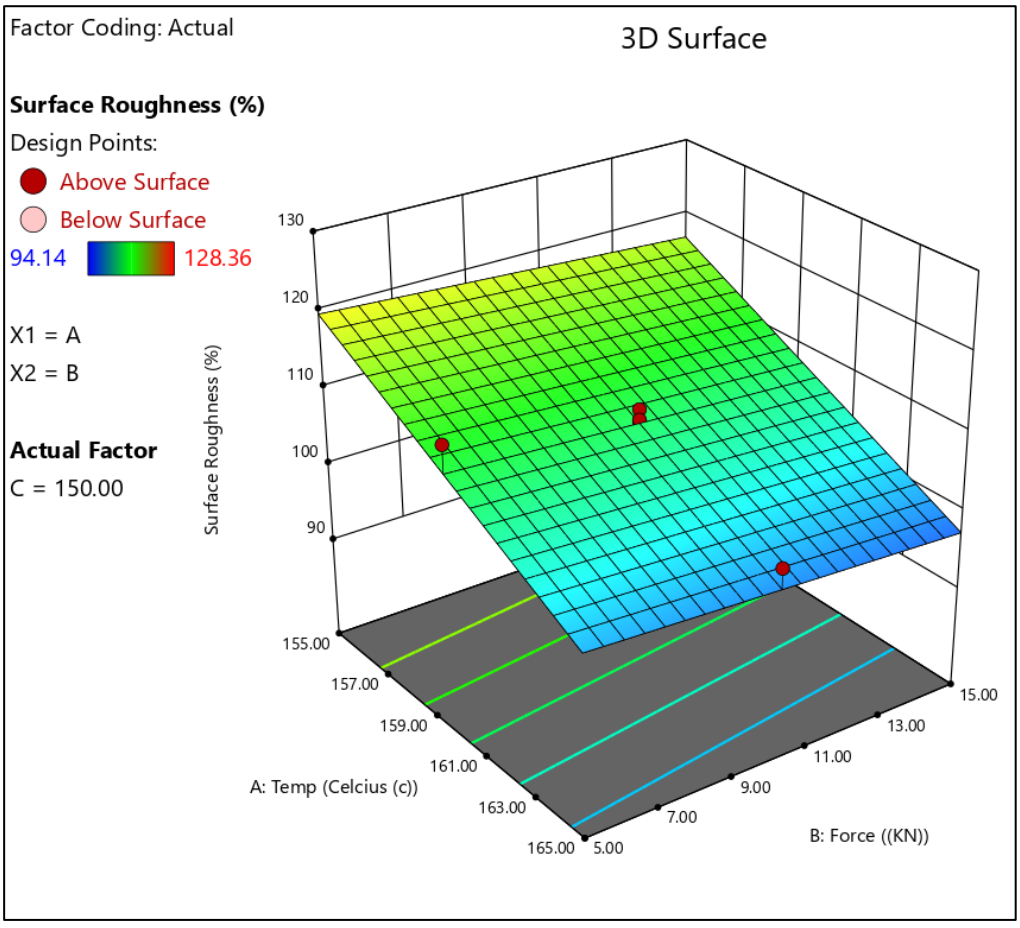

(a)

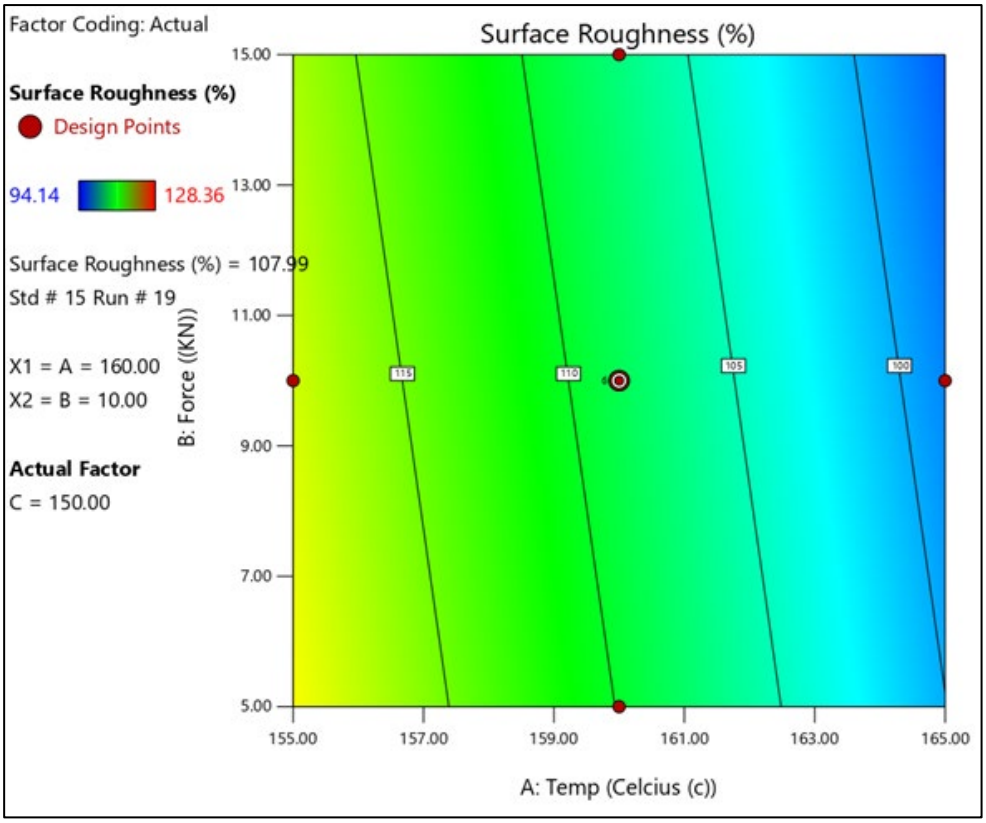

(b)

Fig. 11. Influence of temperature and force on surface roughness quality on HDPE substrate (a) 3D surface plot (b) contour plot

4.5 Parameter's Optimization

As shown in Table 3, the greatest experimental outcomes for each response (temperature, force, and holding time) were obtained at run number 7. Unfortunately, this data shows only the best result for each response, where accuracy is 101.32% and surface roughness is 1.32%. For this reason, the investigation of desirability was carried out to identify the optimal parameters by considering all responses.

Numerical optimization was used using design expert software to discover the design space by utilising mathematical models to determine the factor values that meet the target. The target for dependent variables (substrate accuracy) was set as maximum and surface roughness was set as minimum as desired to acquire the greatest result. Hence, the desirability analysis was chosen to serve as the foundation for the optimization investigations. The geometric (multiplicative) mean of all individual desirability ranging from 0 (least) to 1 is known as the total desirability (*D*). According to the best desirability value, as indicated in Table 6, the ideal set of parameters was selected. The highest desirability value (0.976) reveals the optimization value predicted by RSM is the optimum parameter to gain higher substrate accuracy and surface quality, as seen in Figure 12. Then, these data were used to validate the desirability predictions through an actual experiment. From Table 7, it may be inferred that the projected result is compared with a particular level of desirability, these are the optimum results when all responses are considered. With a maximum error of 2.72%, this result indicates a strong agreement between predicted and experimental results.

Table 6
Prediction of optimum HE temperature, HE force and holding time by RSM

No	Factors			Responses		Desirability
	Embossing Temperature (^{0}c)	Embossing Force (kN/s)	Embossing Holding Time (s)	Depth accuracy (%)	Surface Roughness (%)	
1	165	10.6	200	93.51	93.64	0.976

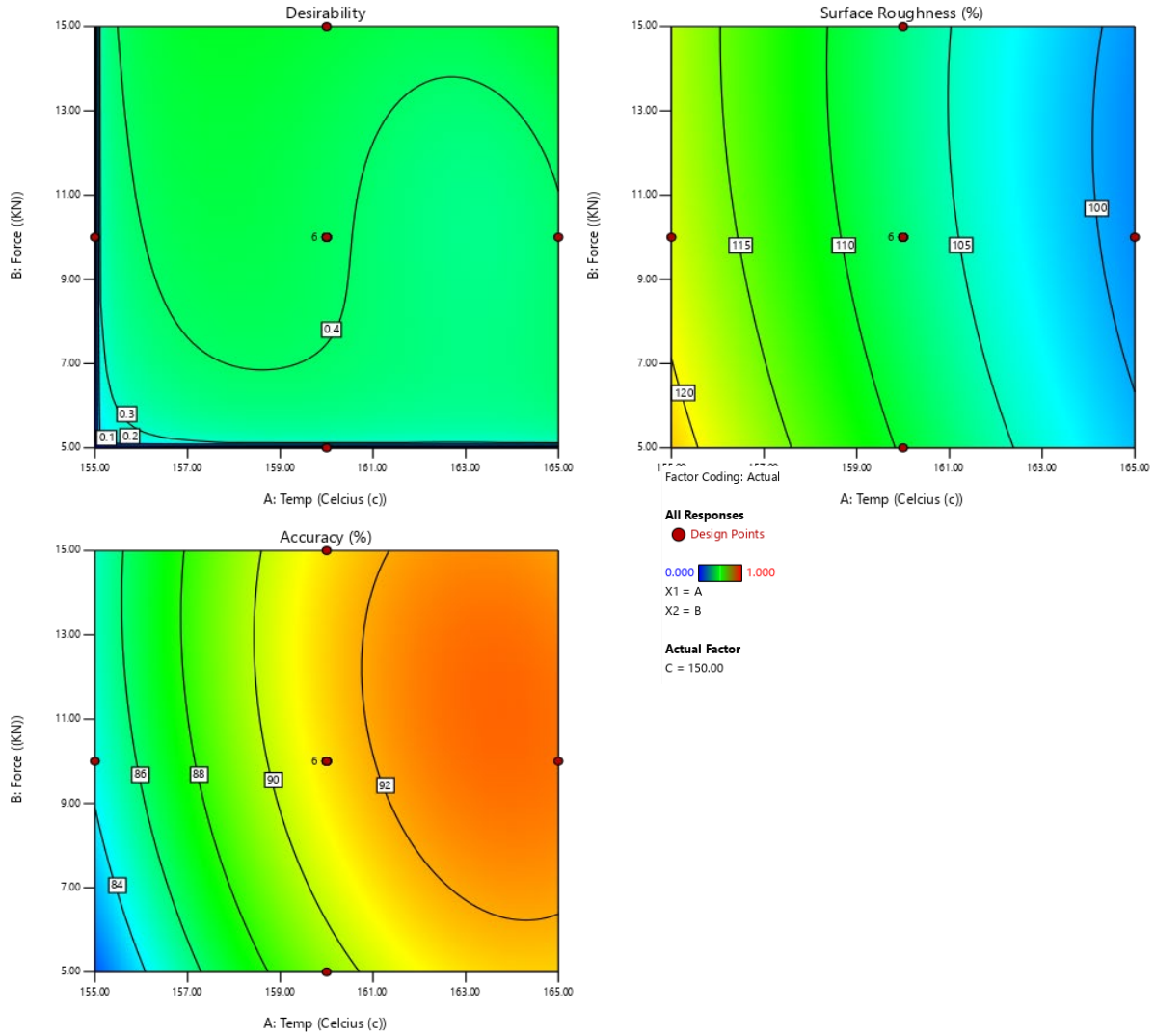

Fig. 12. Desirability plot considering the micro grating accuracy and surface quality

Table 7
Comparison of predicted and experimental results

No	Factors	Desirability	Accuracy (%)			Surface roughness (%)		
			Predicted /(RSM)	Actual /(Exp)	Error/%	Predicted /(RSM)	Actual /(Exp)	Error/%
1	Refer table 6	0.670	93.51	95.59	2.22	93.64	96.19	2.72

5. Conclusion

In this study, the RSM was utilized to study the optimal process parameters that contribute to enhancing the replication accuracy and surface roughness of HDPE micro grating substrate using the

hot embossing technique. Employing RSM helps a researcher to design the experiment plan, parameters selection and analyse the experimental data to distinguish the significant variable that contributes to substrate quality. The data acquired from RSM indicated that the hot embossing (HE) temperature is the main factor for deviation in the dimension of the HDPE substrate structure as compared to other parameters. After investigation, the following conclusion has been derived:

i. The ANOVA contour plot reveals that the replication accuracy of HDPE micro grating substrate is increased from 80.76 % to 94.25% as the increment of HE temperature from 155^{o}c to 165^{o}c.
ii. The percentage of surface roughness decreased from 128.36% to 94.14% when the temperature increased from 155^{o}c to 165^{o}c. The decrease in the surface roughness percentage represents the increase in the surface quality of the substrate.
iii. A greater deviation in substrate structure has been caused by higher embossing temperatures setting (above glass transition). It increases the polymer viscosity and fills in mould space in a viscoelastic condition.
iv. The desirability method of RSM is the best approach to optimised the experiment data. A higher desirability of 97.9% was achieved at the HE temperature of 165^{o}c, HE forces 10.6 kN/s and embossing time of 200 seconds. This data represents the optimum parameter for replication of HDPE substrate using an in-house HE setup.
v. The predicted optimum parameter is then validated through experiment, the maximum error of 2.72% shows the deviation in percentage within a reasonable range.

References

[1] Worgull, M., A. Kolew, M. Heilig, M. Schneider, H. Dinglreiter, and B. Rapp. "Hot embossing of high performance polymers." *Microsystem technologies* 17 (2011): 585-592. https://doi.org/10.1007/s00542-010-1155-0
[2] Peng, Linfa, Yujun Deng, Peiyun Yi, and Xinmin Lai. "Micro hot embossing of thermoplastic polymers: a review." *Journal of Micromechanics and Microengineering* 24, no. 1 (2013): 013001. https://doi.org/10.1088/0960-1317/24/1/013001
[3] Genna, S., Claudio Leone, and V. Tagliaferri. "Characterization of laser beam transmission through a High Density Polyethylene (HDPE) plate." *Optics & Laser Technology* 88 (2017): 61-67. https://doi.org/10.1016/j.optlastec.2016.08.010
[4] Manaf, Ahmad Rosli Abdul, Tsunetoshi Sugiyama, and Jiwang Yan. "Design and fabrication of Si-HDPE hybrid Fresnel lenses for infrared imaging systems." *Optics Express* 25, no. 2 (2017): 1202-1220. https://doi.org/10.1364/OE.25.001202
[5] Kaneda, R., T. Takahashi, M. Takiguchi, M. Hijikata, and H. Ito. "Optical Properties of HDPE in Injection Molding and Injection Press Molding for IR System Lenses." *International Polymer Processing* 31, no. 3 (2016): 385-392. https://doi.org/10.3139/217.3261
[6] Manaf, Ahmad Rosli Abdul, and Jiwang Yan. "Improvement of form accuracy and surface integrity of Si-HDPE hybrid micro-lens arrays in press molding." *Precision Engineering* 47 (2017): 469-479. https://doi.org/10.1016/j.precisioneng.2016.10.002
[7] Manaf, Ahmad Rosli Abdul, and Jiwang Yan. "Press molding of a Si–HDPE hybrid lens substrate and evaluation of its infrared optical properties." *Precision Engineering* 43 (2016): 429-438. https://doi.org/10.1016/j.precisioneng.2015.09.007
[8] Shan, Xuechuan, L. Jin, Y. C. Soh, and C. W. Lu. "A polymer-metal hybrid flexible mould and application for large area hot roller embossing." *Microsystem technologies* 16 (2010): 1393-1398. https://doi.org/10.1007/s00542-009-0991-2
[9] Kaneda, Ryo, Toshihiro Takahashi, Masayasu Takiguchi, Motoharu Hijikata, and Hiroshi Ito. "Optical properties of high-density polyethylene in injection press molding for IR system lenses." *Polymer Engineering & Science* 58, no. 5 (2018): 632-641. https://doi.org/10.1002/pen.24592
[10] Ippolito, Christina, Sufujiang Yu, Yong Jun Lai, and Tim Bryant. "Process parameter optimization for hot embossing uniformly textured UHMWPE surfaces for orthopedic bearings." *Procedia CIRP* 65 (2017): 163-167. https://doi.org/10.1016/j.procir.2017.04.039

[11] Jha, Jyoti Shankar, and Suhas Sitaram Joshi. "Numerical simulation of micro hot embossing of polymer substrate." *International Journal of Precision Engineering and Manufacturing* 13 (2012): 2215-2224. https://doi.org/10.1007/s12541-012-0294-x
[12] Li, J. M., C. Liu, and J. Peng. "Effect of hot embossing process parameters on polymer flow and microchannel accuracy produced without vacuum." *Journal of materials processing technology* 207, no. 1-3 (2008): 163-171. https://doi.org/10.1016/j.jmatprotec.2007.12.062
[13] Chang, Chih-Yuan, and Jia-Hao Chu. "Innovative design of reel-to-reel hot embossing system for production of plastic microlens array films." *The International Journal of Advanced Manufacturing Technology* 89 (2017): 2411-2420. https://doi.org/10.1007/s00170-016-9277-x
[14] Deshmukh, Swarup S., Tuhin Kar, Saikat Som, and Arjyajyoti Goswami. "Investigation of replication accuracy of embossed micro-channel through hot embossing using laser patterned copper mold." *Materials Today: Proceedings* 60 (2022): 2222-2229. https://doi.org/10.1016/j.matpr.2022.03.128
[15] Lan, Shuhuai, Hye-Jin Lee, EunHee Kim, Jun Ni, Soo-Hun Lee, Xinmin Lai, Jung-Han Song, Nak Kye Lee, and Moon G. Lee. "A parameter study on the micro hot-embossing process of glassy polymer for pattern replication." *Microelectronic Engineering* 86, no. 12 (2009): 2369-2374. https://doi.org/10.1016/j.mee.2009.04.023
[16] Moore, Sean, Juan Gomez, Devanda Lek, Byoung Hee You, Namwon Kim, and In-Hyouk Song. "Experimental study of polymer microlens fabrication using partial-filling hot embossing technique." *Microelectronic Engineering* 162 (2016): 57-62. https://doi.org/10.1016/j.mee.2016.05.009
[17] Kuo, C-C., and B-C. Chen. "Optimization of hot embossing molding process parameters of Fresnel lens using Taguchi method: Optimierung von Heißpräge-Spritzguss-Prozessparametern für Fresnel-Linsen mit der Taguchi-Methode." *Materialwissenschaft und Werkstofftechnik* 46, no. 9 (2015): 942-948. https://doi.org/10.1002/mawe.201500443
[18] He, Yong, Jian-Zhong Fu, and Zi-Chen Chen. "Optimization of control parameters in micro hot embossing." *Microsystem technologies* 14 (2008): 325-329. https://doi.org/10.1007/s00542-007-0497-8
[19] Wu, Cheng Hsien, Chen Hao Hung, and Ya Zhen Hu. "Parametric study of hot embossing on micro-holes." *Advanced Materials Research* 74 (2009): 251-254. https://doi.org/10.4028/www.scientific.net/AMR.74.251
[20] Manaf, Ahmad Rosli Abdul, and Jiwang Yan. "Improvement of form accuracy and surface integrity of Si-HDPE hybrid micro-lens arrays in press molding." *Precision Engineering* 47 (2017): 469-479. https://doi.org/10.1016/j.precisioneng.2016.10.002
[21] Wang, Jin, Peiyun Yi, Yujun Deng, Linfa Peng, Xinmin Lai, and Jun Ni. "Recovery behavior of thermoplastic polymers in micro hot embossing process." *Journal of Materials Processing Technology* 243 (2017): 205-216. https://doi.org/10.1016/j.jmatprotec.2016.12.024
[22] Chen, Xi, Zhiqiang Wei, Lei Zhu, Xing Yuan, Daneng Wei, Wei Peng, and Chunjie Wu. "Efficient approach for the extraction and identification of red pigment from zanthoxylum bungeanum maxim and its antioxidant activity." *Molecules* 23, no. 5 (2018): 1109. https://doi.org/10.3390/molecules23051109
[23] G. Derringer and R. Suich, "Simultaneous Optimization of Several Response Variables," Journal of Quality Technology, vol. 12, no. 4, pp. 214–219, Oct. 1980, doi: 10.1080/00224065.1980.11980968.
[24] Deshmukh, S. S., and A. Goswami. "Investigation of deviation in width of embossed micro-structure by hot embossing." In *IOP Conference Series: Materials Science and Engineering*, vol. 872, no. 1, p. 012069. IOP Publishing, 2020. https://doi.org/10.1088/1757-899X/872/1/012069
[25] Khalil, Khair, A. Mohd, C. O. C. Mohamad, Y. Faizul, and S. Zainal Ariffin. "The Optimization of Machining Parameters on Surface Roughness for AISI D3 Steel." In *Journal of Physics: Conference Series*, vol. 1874, no. 1, p. 012063. IOP Publishing, 2021. https://doi.org/10.1088/1742-6596/1874/1/012063
[26] Deshmukh, Swarup S., and Arjyajyoti Goswami. "Hot Embossing of polymers–A review." *Materials Today: Proceedings* 26 (2020): 405-414. https://doi.org/10.1016/j.matpr.2019.12.067
[27] Askins, Steve, Marta Victoria, Rebeca Herrero, César Domínguez, Ignacio Antón, and Gabriel Sala. "Effects of temperature on hybrid lens performance." In *AIP Conference Proceedings*, vol. 1407, no. 1, pp. 57-60. American Institute of Physics, 2011. https://doi.org/10.1063/1.3658294
[28] Xiong, Hao, Linjue Wang, and Zheyao Wang. "Chalcogenide microlens arrays fabricated using hot embossing with soft PDMS stamps." *Journal of Non-Crystalline Solids* 521 (2019): 119542. https://doi.org/10.1016/j.jnoncrysol.2019.119542